IEEE Access
Multidisciplinary ⋮ Rapid Review ⋮ Open Access Journal

Received 24 April 2024, accepted 21 May 2024, date of publication 28 May 2024, date of current version 4 June 2024.

Digital Object Identifier 10.1109/ACCESS.2024.3406632

RESEARCH ARTICLE

An Investigation of Optimized Carbon Tax-Subsidy Mechanism to Enhance Power System Sustainability Considering Wind Power Penetration

NIMA SHAFAGHATIAN, SEYED HADI HOSSEINI, AND REZA NOROOZIAN
Department of Electrical Engineering, Faculty of Engineering, University of Zanjan, Zanjan 4537138791, Iran
Corresponding author: Reza Noroozian (noroozian@znu.ac.ir)

ABSTRACT In addressing current sustainability challenges, it is crucial to reduce CO_2 emissions from power systems. An economic approach is to devise a solution for increasing the penetration of renewable energy sources. This can be achieved by implementing taxes on CO_2 emissions from fossil fuel power plants (FFPP). However, it is important to carefully design this tax to ensure that sustainability is not compromised. For instance incorrect tax amounts and implementation methods can result in an excessive increase in energy prices and a reduction in consumption. This paper proposes the power system sustainability index (PSSI), which incorporates economic, social and environmental aspects to obtain optimal tax. Furthermore, tax revenue is allocated as a subsidy to wind power plants (WPP). The mutual effects of taxation, prices and subsidies create a loop, wherein the amount paid as a subsidy and received as tax converge in an optimized cycle. Thus, the proposed optimized carbon tax-subsidy mechanism (OCTSM) has two key characteristics: it increases the PSSI optimally and ensures equivalence between the amounts paid and received. The effectiveness of the developed strategy was evaluated on the modified IEEE 24-bus test system with penetration of WPP along with power production uncertainties. The results indicate that an optimized tax system leads to a higher PSSI. Furthermore, as the total installed capacity of WPP increases, the impact of the tax on improving the PSSI becomes even more significant. However, there is a limit to the capacity expansion, beyond which the effect on the PSSI diminishes.

INDEX TERMS Carbon tax, energy policy, power system sustainability, tax-subsidy mechanism, wind power penetration.

NOMENCLATURE

A. INDICES AND SETS

i	Index of power plants.
h	Index of time slots.
F	Index of fossil fuel power plants.
w	Index of wind power plants.
k	Index of the wind scenarios.
s	Index of the system.
b	Index of the buses of the system.
j	Index of the system convergence iterations.
n_F	number of fossil fuel power plants.
n_W	number of wind power plants.
aft	After OCTSM.
bef	Before OCTSM.

The associate editor coordinating the review of this manuscript and approving it for publication was Hamdi Abdi.

B. PARAMETERS

a_{F_i}	The non-linear coefficient in the cost function of fossil fuel power plants.

β_{F_i}	The linear coefficient in the cost function of fossil fuel power plants.
γ_{F_i}	The start-up cost factor of fossil fuel power plant.
a_{w_i}	The non-linear coefficient is a function of the cost of wind plants.
β_{w_i}	The linear coefficient is a function of the cost of wind plants.
γ_{w_i}	The start-up cost factor of a wind power plant.
n	The predetermined percentage for the allocation of subsidies of the total amount of tax.
τ	A small threshold value which convergence in inner loop is achieved when the difference between the taxation amount and the subsidy is less than that.
σ	A small threshold value which convergence in outer loop is achieved when the difference between the total demands is less than that.
ε	Price elasticity.
N_{Gl}	number of genes.

C. VARIABLES

$C^{bef}_{F_{i,h}}$	The cost function of the i^{th} fossil fuel power plant at hour h before tax.
$C^{aft}_{F_{i,h}}$	The cost function of the i^{th} fossil fuel power plant at hour h after tax.
$C^{bef}_{w_{i,h}}$	The cost function of the i^{th} wind power plant at hour h before applying tax.
$C^{aft}_{w_{i,h}}$	The cost function of the i^{th} wind power plant at hour h after applying tax.
$C^{aft}_{w_{i,h,j+1}}$	The cost function of the i^{th} wind power plant at hour h in the $j+$ 1st iteration of subsidy allocation.
$P_{F_{i,h}}$	The power produced by the i^{th} fossil fuel power plant at hour h.
$P_{w_{i,h}}$	The power produced by the i^{th} wind power plant at hour h.
$P_{w_{i,h,j+1}}$	The power produced by the wind power plant at hour h in the $j+1$th iteration subsidy allocation.
$tax_{i,h}$	Tax formula for the i^{th} producer in hour h.
$PSSI$	Power system sustainability index.
w_{CO_2}	Tons of CO_2 emission.
D	Electricity total demand.
F_{CO_2}	A coefficient to equate the social cost of carbon in dollars (\$/ton).
F_D	A coefficient to equate the demand in dollars (\$/MW).
R_{CO_2}	Tons of CO_2 emission per MWh (ton/MWh).
$aveLMP$	Average 24-hour locational marginal price.
F_{tax_t}	Total revenue made from tax.
S_t	The total amount of subsidy for wind generators in 24 hour.
S_o	The total amount of revenue obtained from the tax after 24 hour.
S_w	Amount of subsidy for each wind generator in 24 hour.
a_{tax}	The non-linear coefficient in the tax formula.
β_{tax}	The linear coefficient in the tax formula.
x_{min}, x_{max}	bounds include reference bus angles, voltage magnitudes, and generator injections.
P_k	The probability of occurrence of the k^{th} wind scenario.
$P_{w,k}$	The probable wind power corresponding to *the* k^{th} wind scenario.
$CO_{2,k}$	The probable CO_2 corresponding to *the* k^{th} wind scenario.
CO_{2_b}	Total CO_2 produced by bus b.
$CO_{2_{i,h}}$	CO_2 produced by i^{th} power plant per hour.
UR_i	Ramp up limit of i^{th} producer.
DR_i	Ramp down limit of i^{th} producer.
$P_{i,total}$	Total active power.
$P_{d,total}$	Total active power demand.
$P_{l,total}$	Total active power loss.
$Q_{i,total}$	Total reactive power.
$Q_{d,total}$	Total reactive power demand.
$Q_{l,total}$	Total reactive power loss.
$v^{i,min}_m, v^i_m, v^{i,max}_m$	Minimum, actual, and maximum voltage magnitudes of buses, respectively.
$p^{i,min}_g, p^i_g, p^{i,max}_g$	Minimum, actual, and maximum active power of producers, respectively.
$q^{i,min}_g, q^i_g, q^{i,max}_g$	Minimum, actual, and maximum reactive power of producers, respectively.
θ^{ref}_i θ_i	Nodal voltage angle reference and nodal voltage angle of bus b respectively.
$CP_{F_{i,h}}$	The production cost of fossil fuel power plants per hour.
$CP_{w_{i,h}}$	The production cost of wind plants per hour.
CF	Cost function.

I. INTRODUCTION

Climate change is one of the major problems of the international community. CO_2 emissions from fossil fuel power plants (FFPP) will contribute to rising global temperatures and climate change [1]. Given the importance of environmental issues and the significant impact of the electricity industry, it is essential to develop new management strategies to control CO_2 production in this sector.

Various studies have investigated this issue. Some have focused on monitoring CO_2 emissions in systems with different energy sources (energy hubs), analyzing the flow of carbon emissions among these sources [2], [3]. In [3], this issue has been investigated only considering the electricity network, and the amount and circumstances of carbon emission from generation to consumption have been studied. The study emphasized the crucial role of the demand side in CO_2 production.

Another category, proposes methods for energy management and optimized power flow (OPF) to reduce CO_2 emissions. These methods incorporate CO_2 reduction as a constraint or the primary goal in problem formulation. For instance, in [4], economic dispatch was performed by considering carbon capture and storage systems. Results indicated that integrating carbon capture and storage alongside conventional generation units significantly reduced CO_2 emissions. Energy management was tackled by simultaneously considering energy and carbon prices [5]. Results showed that an increase in the prices led to a decrease in the carbon emissions but with a saturation effect. In [6], operational perspectives were explored, such as studying the appropriate power flow of a system in relation to taxes and uncertainty of energy sources based on improved wild horse optimizer. Results indicated that the proposed method is highly effective and robust in achieving the optimal solution. An optimal interaction between operators and investors within an energy hub system, taking carbon constraints and carbon tax into account, was defined in [7]. Results showed that a taxation-based approach increases total costs of the system at moderate emissions targets, but the effect decreases at aggressive targets. The impact of using different distributed generation sources on greenhouse gas emissions was also examined in [8]. The findings indicated that renewable energy consumption causes economic growth as well as CO_2 emissions. In [9], the impact of CO_2 reduction policies at the provincial level was studied on a case study in China, particularly focusing on circular economy development and energy intensity targets. Interestingly, the findings show that provincial energy saving and comprehensive resource utilization policies do not significantly affect CO_2 emissions.

In [10] the impact of strict penalty-based policies on carbon emissions in highly polluted countries was investigated. By utilizing nonlinear modeling, the study concluded that despite the positive and negative effects associated with implementing these policies, they would ultimately lead to improved environmental conditions in the long term. In [11], incentive instructions were defined for both production and consumption. The results demonstrated that inappropriate policies for distributed generation sources may lead to electricity generation shortages, highlighting the need for an appropriate strategy.

Another category of articles focuses on CO_2 taxation. These studies are divided into two main areas: decision-making in the electricity market environment assuming the existence of taxes, and the impact of different taxes on the operation and planning processes. In the first category, a certain tax amount is typically assumed. For example, the Brookings Institute suggested a minimum carbon tax value of \$15/tonCO_2 [12]. Other studies proposed values ranging from \$15/tonCO_2 to \$29/tonCO_2 [13], or \$10/tonCO_2 up to \$25/tonCO_2 [14]. Several articles have examined the optimal decision-making of market players concerning taxation. For example, [15] presented a model for supply chain decision-making under carbon taxes and constraints, outlining an optimal supply chain. The results indicated that emission reductions and economic benefits can be achieved over time. In [16] the optimal decision-making in the presence of carbon tax was studied in a case study in Taiwan. Key findings include optimized portfolio allocation for green energy projects, contributing to Taiwan's national energy policy, and demonstrating the effectiveness of smart green energy planning incorporating a carbon tax policy for sustainable environmental activities. [17] has studied the optimal pricing for market players in the context of market uncertainty and taxes. Results indicated that while carbon tax can effectively lower carbon emissions, industries with smaller profit margins may face challenges in business development if solely reliant on this policy, potentially resulting in diminished benefits. In [18] a market including one manufacturer and two retailers was studied in terms of carbon tax, where competitive or cooperative policies were examined, highlighting taxation as a useful and effective environmental policy. The main results highlighted that reduced manufacturer or retailer power led to lower profits and in a vertical Nash setup, retail prices were lowest, supply chain demand was highest, and supply chain profit was maximized.

In the second category, the objective is to determine the optimal tax rate by observing its impact on the system while varying its value. For instance, in [19], researchers studied the short-term economic and environmental effects of carbon taxation on bulk electrical systems using various tax rates. The results showed that high taxes on the production side led to higher equilibrium prices and reduced consumption, negatively impacting power system sustainability. In [20], the minimum appropriate tax rate for CO_2 reduction was studied by defining the desired pollution reduction level and deriving the corresponding tax rate. Case studies on a modified ISO New England test system demonstrated the reliability of this method in identifying the minimum tax rate required to meet emissions targets. In [21] a case study was conducted in China to identify an appropriate tax rate. The results showed that the suitable carbon tax was 60 RMB/t, which not only achieved the emission reduction target but also minimized the negative impact on the macroeconomy. Moreover, [22] examined the impact of changing tax rates on the consumption of renewable power plants. The paper indicated that in the short term, environmental tax negatively impacted renewable energy consumption. However, in the long run, a 1% increase in the tax yielded a 1.201% increase in renewable energy consumption. In [23], different reasonable tax rates were also analyzed, along with their influence on the system and environmental pollution levels, providing recommendations for proper system management and coordination. Results showed that a win-win situation was attained for all participants with the proposed coordination scheme, resulting in noticeable reductions in total cost and carbon dioxide emissions. Some researchers also explored the effects of different taxes on system planning across various time horizons.

These studies focused on system expansion planning by considering different tax amounts allocated to carbon reduction in the planning process [24], [25]. The findings of this researches demonstrated the positive impact of allocating taxes towards establishing a framework for planning systems with lower CO_2 emissions. Also, the carbon tax policy is more efficient in reducing CO_2 emissions compared to the renewable portfolio standard (RPS) policy. Additionally, certain articles in this category examined taxes and system planning with constraints on maximum carbon emissions in the target year [26], [27]. Both papers demonstrated that policy carbon taxes played a crucial role in driving the transition to renewable energy and achieving emissions reduction targets. Additionally, they emphasized the importance of optimizing renewable energy deployment strategies to ensure cost efficiency and successful decarbonization of the power sector.

Many references have also proposed addressing the respective discussion with the definition of suitable objective functions and solving them using metaheuristic optimization algorithms.

For instance, references [6] employed an improved wild horse optimizer for optimal power flow in the presence of taxes, while reference [7] utilized neighbor search. The optimal point was obtained by these algorithms in both references. Other references have also utilized optimization algorithms including genetic algorithm (GA) on this topic. In [28] a multi-objective optimization problem in an integrated power generation system in the presence of taxes was solved using GA. The results indicated that this algorithm has successfully converged the problem. Additionally, [29] examined joint decision-making between manufacturers and retailers in supply chains, using GA and considering carbon taxes. In [30] a system planning problem considering tax issues using the same algorithm, was studied. In the mentioned papers, the GA has successfully achieved convergence for the proposed problem.

To the best of the authors' knowledge, no prior studies have examined the determination of the optimal tax and its allocation method to maximize power system sustainability. This paper aims to address this gap by introducing a power system sustainability index (PSSI) and investigating an optimized carbon tax-subsidy mechanism (OCTSM) that maximizes it by appropriate increase in penetration of renewable sources. Furthermore, this study also conducted an analysis of the relationship between wind generator installed capacity and the enhancement of PSSI through the implementation of OCTSM. The GA has been utilized to solve the relevant objective function. This algorithm has demonstrated satisfactory performance in similar articles and has been chosen for implementation due to its simplicity, high prevalence and effectiveness.

TABLE 1. Classification of reviewed papers.

Symbol	References
Impact of taxes on system planning	[24], [25], [26], [27]
Effect of taxes on system and CO_2 emission	[13], [19], [20], [21], [22], [23]
Decisions of market players in terms of taxation	[15], [16], [17], [18]
policies on CO_2 emissions	[8], [9], [10], [11]
Load distribution or power flow considering CO_2 emissions	[4], [5], [6], [7],
Monitoring the amount of CO_2	[2], [3]
OCTSM according to power system sustainability	Proposed Method

The reviewed papers along with the proposed method have been classified in Table 1. The methodology involves a mathematical model and an iterative process. The study has been conducted on the enhanced IEEE 24-bus test system with wind power plants (WPP).

The remaining sections of this paper are organized as follows: Section II describes the proposed PSSI and the layout of OCTSM, while the formulation of the proposed OCTSM is defined in Section III. Section IV describes the obtained results and a comprehensive discussion. Finally, Section V presents the conclusions.

II. POWER SYSTEM SUSTAINABILITY INDEX FOR THE PROPOSED OCTSM

In this section, the definition of PSSI is described based on the general definition of sustainability, followed by the layout and implementation of OCTSM in the examined problem.

A. PROPOSED PSSI

Sustainability involves addressing critical limits related to environmental degradation and pursuing competitive objectives that prioritize a balance between social, economic, and environmental factors [31]. These factors influence each other, ultimately impacting sustainability. In this study, an approach has been taken to mitigate carbon dioxide emissions and uplift sustainability by imposing OCTSM. The related sustainability indicators in this context, which define PSSI, are selected according to [31] and [32]. Fig. 1 illustrates the impact of taxes and subsidies on the PSSI indicators. These indicators include cost, price, consumption, and CO_2 emissions that are presented as an objective function in section III. The tax and subsidy change the cost function of power plants, which in turn impacts the results of the OPF and system outputs, and consequently the PSSI indicators. The OCTSM is designed to promote the penetration of WPP in a way that aligns with the overall objective of increasing PSSI.

B. LAYOUT OF THE PROPOSED METHOD

The overall layout of the proposed method is illustrated in Fig. 2, which provides a visual representation of the general

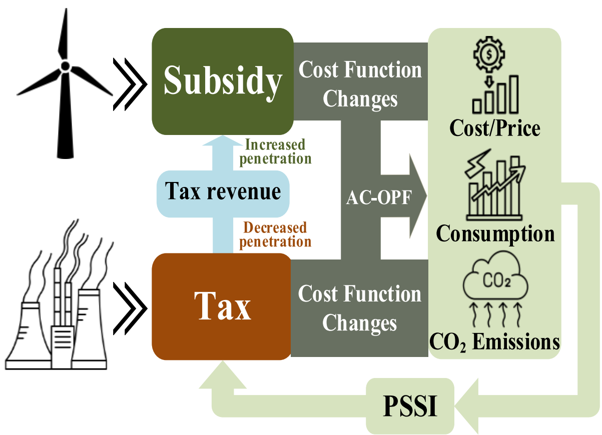

FIGURE 1. Placement of PSSI and related indicators in the proposed method.

concept. The OCTSM processing, performed by the financial authority, takes into account the cost functions of power plants, system structure, load profiles, and other factors such as demand elasticity and wind scenarios. In the processing operation, the determined tax through an algorithm, causes a change in the cost function of FFPP. By applying AC-OPF, the network price and the amount obtained from taxation are determined. A portion of this amount is allocated as a subsidy to wind generators, impacting their cost function. As a result, a different amount from taxation will be obtained through the power flow (due to the increased penetration of WPP). This means that the subsidy provided to WPP does not equal the taxation amount. This process continues until convergence is achieved, equalizing the subsidy and taxation amounts. After the convergence of the inner loop, price-based demand response (PBDR) is applied, leading to a change in the consumption. This triggers another execution of the inner loop, considering the change in price. Finally, with the convergence of the outer loop, the final values of consumption, network price, and emitted carbon dioxide are obtained, determining the level of PSSI based on (8). This process is optimized using GA to obtain the OCTSM that maximizes PSSI. It should be noted that any types of renewable power plants can be studied instead of WPP without loss of generality.

III. FORMULATION OF THE PROPOSED OCTSM

In this section, the problem formulation is presented. The section further explores and formulates the uncertainty of wind production, PBDR model, and the solution technique.

A. FORMULATION OF THE PROPOSED METHOD

The cost function of power plants is represented by a non-linear equation:

$$C^{bef}_{F_{i,h}} = a_{F_i} P^2_{F_{i,h}} + \beta_{F_i} P_{F_{i,h}} + \gamma_{F_i} \tag{1}$$

Here, $C^{bef}_{F_{i,h}}$ is the cost function of the i^{th} FFPP at hour h before tax, $P^2_{F_{i,h}}$ is the power produced by the i^{th} FFPP at hour h;a_{F_i}, β_{F_i} and γ_{F_i} are the non-linear, linear and start-up cost factors of i^{th} FFPP respectively.

The values of a_{F_i}, β_{F_i} and γ_{F_i} are obtained from [33]. The amount of carbon dioxide emitted is proportional to the power produced by FFPP [34]. The basic formulation for taxation is as follows:

$$tax_{i,h} = f(generatedCO_{2_{i,h}}) = f(g(P_{F_{i,h}})) = \mathscr{L}(P_{F_{i,h}}) \tag{2}$$

where $tax_{i,h}$ is the tax formula for the i^{th} producer in hour h, $CO_{2_{i,h}}$ is the CO_2 produced by i^{th} FFPP in hour h and $P_{F_{i,h}}$ is the power produced by the i^{th} FFPP at hour h. According to (2), the tax rate is a function of the carbon dioxide emissions, which itself is a function of the power generation capacity of FFPP. In this paper, a non-linear tax to account for the increase in pressure with production has been considered. As many sources have recommended this method, including [35]. So (2) can be written as follows:

$$tax_{i,h} = a_{tax} P^2_{F_{i,h}} + \beta_{tax} P_{F_{i,h}} \tag{3}$$

where, a_{tax} and β_{tax} demonstrate the non-linear and linear coefficients of the tax formula respectively. In order to compensate for the impact of the tax, generators adjust their cost functions by increasing costs. Therefore, based on (1) and (3):

$$C^{aft}_{F_{i,h}} = (a_{F_i} + a_{tax}) P^2_{F_{i,h}} + (\beta_{F_i} + \beta_{tax}) P_{F_{i,h}} + \gamma_{F_i} \tag{4}$$

where $C^{aft}_{F_{i,h}}$ is the cost function of the i^{th} FFPP at hour h after tax. The objective function aims to maximize the PSSI by considering costs, carbon dioxide emissions, and consumption according to section II, and the respective cost function is formulated as follows:

$$CF = (\sum_{i=1}^{n_F} \sum_{h=1}^{24} CP_{F_{i,h}} + \sum_{i=1}^{n_W} \sum_{h=1}^{24} CP_{w_{i,h}}) + (\sum_{i=1}^{n_F} \sum_{h=1}^{24} w_{CO_{2_{i,h}}}) F_{CO_2} - D_s \times F_D \tag{5}$$

Here, CF demonstrates the cost function, $CP_{F_{i,h}}$ and $CP_{w_{i,h}}$ are the cost of FFPP and WPP per hour respectively. $w_{CO_{2_{i,h}}}$ is the Tons of CO_2 emission of i^{th} FFPP at hour h, D_s is the Electricity total demand and F_D is a coefficient to equate the demand in dollars (\$/MW). F_{CO_2} represents a coefficient that equates the number of tons of CO_2 produced by power plants to the corresponding environmental costs. In other words, the cost of producing 1 ton of CO_2 is F_{CO_2} dollars. The amount of CO_2 emission is a linear function of power plant production as follows:

$$\mathrm{w_{CO_{2_{i,h}}}} = \mathrm{R_{CO_2} P_{F_{i,h}}} \tag{6}$$

where R_{CO_2} is the Tons of CO_2 emission per MWh (ton/MWh). The overall PSSI of the system, based on the objective function, can be defined as follows:

$$PSSI_s = \frac{CF^{bef}}{CF^{aft}} \tag{7}$$

where $PSSI_s$ is the power system sustainability index, CF^{bef} and CF^{aft} are the cost functions before and after tax respectively. After the tax is imposed, the power generated by FFPP

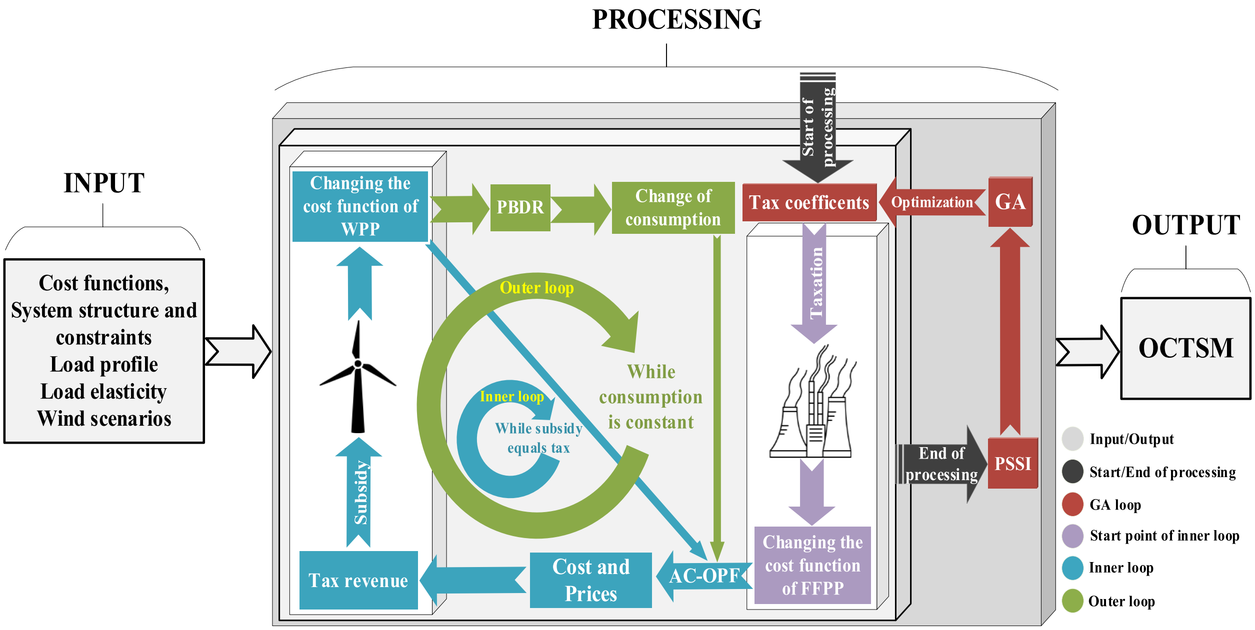

FIGURE 2. Overall layout of the proposed OCTSM.

and CO_2 emissions is decreased. This reduction is a result of the increased price of these plants. The PSSI can also be calculated for each bus. The following general equation can calculate PSSI index in different buses:

$$PSSI_b = \frac{aveLMP_b^{bef}}{aveLMP_b^{aft}} + \frac{\sum_{h=1}^{24} W_{CO_{2b,h}}^{bef}}{\sum_{h=1}^{24} W_{CO_{2b,h}}^{aft}} - \frac{\sum_{h=1}^{24} D_{b,h}^{bef}}{\sum_{h=1}^{24} D_{b,h}^{aft}} \quad (8)$$

$W_{CO_{2b,h}}^{bef}$ and $W_{CO_{2b,h}}^{aft}$ are the tons of CO_2 emission from b^{th} bus in hour h before and after tax respectively, and $D_{b,h}^{bef}$ and $D_{b,h}^{aft}$ are the Electricity demands in b^{th} bus before and after tax respectively. It also should be noted that the $PSSI_b$ is not defined for buses that neither generate CO_2 emissions nor consume energy.

The main objective is to increase the $PSSI_s$ as outlined in (8), with the $PSSI_b$ of individual buses being the dependent outputs. The following equation is utilized to determine the tax rate:

$$F_{tax_t} = \sum_{i=1}^{n_F} \sum_{h=1}^{24} tax_{i,h} \quad (9)$$

where F_{tax_t} is the total revenue made from tax and can be allocated as a subsidy to wind generators. Various percentages for the allocation of this subsidy can be examined. The subsidy amount is obtained as follows:

$$S_t = \%n\ F_{tax_t} \quad (10)$$

where S_t is the total amount of subsidy for wind generators in 24 hours and %n is a predetermined percentage for the allocation of subsidies of the total amount of tax.

It is important to note that S_t represents the considered subsidy amount, which is distinct from the amount obtained at the end of 24 hours (S_o). As S_t affects the cost functions of the wind turbines, it consequently impacts the AC-OPF and the tax amount. To address this interdependency, a converging loop is taken into account.

The subsidy amount for each wind generator is as follows:

$$S_{w_{i,h}} = \frac{S_t}{\sum_{i=1}^{n_w} \sum_{h=1}^{24} P_{w_{i,h}}} \quad (11)$$

where $S_{w_{i,h}}$ is the amount of subsidy for i^{th} wind generator in hour h.

The cost function of wind generators, similar to FFPP, is as follows:

$$C_{w_{i,h}}^{bef} = a_{w_i} P_{w_{i,h}}^2 + \beta_{w_i} P_{w_{i,h}} + \gamma_{w_i} \quad (12)$$

Here, $C_{w_{i,h}}^{bef}$ is the cost function of the i^{th} WPP at hour h before tax, $P_{w_{i,h}}^2$ is the power produced by the i^{th} WPP at hour h;a_{w_i}, β_{w_i} and γ_{w_i} are the non-linear, linear and start-up cost factors of i^{th} WPP respectively. By applying subsidy to wind generators, cost functions change as follows:

$$C_{w_{i,h}}^{aft} = a_{w_i} P_{w_{i,h}}^2 + (\beta_{w_i} - S_{w_{i,h}}) P_{w_{i,h}} + \gamma_{w_i} \quad (13)$$

where $C_{w_{i,h}}^{aft}$ is the cost function of the i^{th} WPP at hour h after tax. A notable point is the change in the share of wind production and its increase after the allocation of subsidies. Based on Fig. 2, this will have an impact on the F_{tax_t}, and consequently, S_t according to (10). As a result, the subsidy amount for WPP will change, along with their cost functions, as indicated in (11) and (13). Consequently, (13) can be rewritten as follows:

$$C_{w_{i,h,j+1}}^{aft} = a_{w_i} P_{w_{i,h,j+1}}^2 + (\beta_{w_i} - S_{w_{ij}}) P_{w_{i,h,j+1}} + \gamma_{w_i} \quad (14)$$

where, j is the counter of iterations until it reaches a permanent state and converges.

After performing the AC-OPF, the power of WPP, i.e., $P_{w_{i,h,j+1}}$ and also the power of FFPP, i.e., $P_{F_{i,h,j+1}}$ is obtained. Consequently , $S_{w,h,j+1}$ is calculated. This iterative process continues until the system converges and reaches a stable state. Once convergence is achieved, the final allocation of power plants and the value of SW_s can be determined. The suggested steps for the proposed method can be summarized as follows:

Step1: Forecast tomorrow's demand.

Step2: Determine the tax based on (3).

Step3: Adjust the cost functions of FFPP according to (4).

Step4: Run the AC-OPF

Step5: The current iteration is j.

Step6: Calculate F_{tax_t} according to (9).

Step7: Calculate wind subsidies according to (11).

Step8: Adjust the cost functions of WPP according to (14).

Step9: Increment j by 1.

Step10: if %n $F_{tax_t} - S_o < \tau$, proceed to step 11; otherwise, return to step 4.

Step11: Perform PBDR and adjust the demand.

Step12: if $D_{s,j} - D_{s,j-1} < \sigma$, proceed to step 13; otherwise, return to step 4.

Step13: Obtain the final tax that meets both optimality and convergence criteria for the subsidy amounts.

B. WIND POWER UNCERTAINTY

The output power of a wind turbine is a function of wind speed and is subject to uncertainty. Therefore, a probabilistic modelling approach is employed, as described in [36] and [37]. The probability distribution of different wind speeds is modelled using the Weibull distribution and discretized into various wind scenarios. The AC-OPF considers the maximum obtainable power for each scenario, which is then adjusted based on the corresponding probabilities. Consequently, the potential output of wind power is adjusted as follows:

$$P_{w_{i,h}} = \int_{1}^{K} P_k P_{w_{i,h,k}} dk \tag{15}$$

where, P_k is the probability of occurrence of the k^{th} wind scenario. After discretization, the obtained result is as follows:

$$P_{w_{i,h}} = \sum\nolimits_{1}^{K} P_k P_{w_{i,h,k}} \tag{16}$$

The amounts of CO_2, as well as the production costs of both WPP and FFPP, are modified as follows:

$$w_{CO_{2_{i,h}}} = \sum\nolimits_{1}^{k} P_k w_{CO_{2_{i,h,k}}} \tag{17}$$

$$CP_{w_{i,h}} = \sum\nolimits_{1}^{K} P_k CP_{w_{i,h,k}} \tag{18}$$

$$CP_{F_{i,h}} = \sum\nolimits_{1}^{K} P_k CP_{F_{i,h,k}} \tag{19}$$

Therefore, the cost function in (5) is rewritten as follows:

$$CF = \sum\nolimits_{1}^{K} P_k((\sum\nolimits_{i=1}^{n_F} \sum\nolimits_{h=1}^{24} CP_{F_{i,h}} + \sum\nolimits_{i=1}^{n_W} \sum\nolimits_{h=1}^{24} CP_{w_{i,h}}) + (\sum\nolimits_{i=1}^{n_F} \sum\nolimits_{h=1}^{24} w_{CO_{2_{i,h}}})F_{CO_2} - D_s \times F_D) \tag{20}$$

It should be noted that scenario generation methods based on wind data and scenario reduction methods should be applied to reduce the computational burden. These methods are employed to generate a representative set of scenarios that capture the uncertainty in wind power generation.

C. PBDR MODEL

PBDR is the reaction of the electricity demand to pricing signals. It reflects the tendency of the load to adjust its consumption patterns based on the prevailing electricity prices. This paper uses the *price elasticity* matrix of *demand* which is an economic term used to discuss price sensitivity. In this model, the electricity price elasticity matrix is used to represent the demand variation resulting from price adjustments. The price elasticity can be calculated as follows [38]:

$$\varepsilon = \frac{\Delta D/D}{\Delta \rho/\rho} \tag{21}$$

Here, ΔD and $\Delta \rho$ represent the percentage increments in electricity demand (D) and price (ρ), respectively.

In the multi-time intervals response model, electricity elasticity coefficients can be categorized as self-elasticity coefficient and mutual elasticity coefficient. Based on the definition in (21), the self-elasticity coefficient and mutual elasticity coefficient can be defined as (22) and (23), respectively:

$$\varepsilon_{i,i} = \frac{\Delta D_c/\mathrm{D}_c}{\Delta \rho_c/\rho_c} \tag{22}$$

$$\varepsilon_{i,j} = \frac{\Delta D_c/\mathrm{D}_c}{\Delta \rho_v/\rho_v} \tag{23}$$

Here, the subscripts c and v represent the c_{th} and v_{th} intervals, respectively. The model for PBDR can be expressed as:

$$\begin{pmatrix} \Delta q_1/\mathrm{q}_1 \\ \Delta q_2/\mathrm{q}_2 \\ \vdots \\ \Delta q_n/\mathrm{q}_n \end{pmatrix} = E \begin{pmatrix} \Delta p_1/p_1 \\ \Delta p_2/p_2 \\ \vdots \\ \Delta p_n/p_n \end{pmatrix} \tag{24}$$

Here E represents the electricity elasticity matrix which is:

$$E = \begin{pmatrix} \varepsilon_{11} & \cdots & \varepsilon_{1n} \\ \vdots & \ddots & \vdots \\ \varepsilon_{n1} & \cdots & \varepsilon_{nn} \end{pmatrix} \tag{25}$$

D. SOLUTION TECHNIQUE

The use of meta-heuristic search algorithms, such as GA, is widespread due to their numerous advantages. One key advantage is that they do not require the problem to be formulated mathematically. In the proposed problem, GA is employed as the solution method. Each chromosome has a number of genes equal to the number of coefficients in the tax formula. In the case of a non-linear tax (as considered in this paper), each chromosome will have two genes. The algorithm is responsible for determining these genes.

Therefore, the number of genes can be calculated using the following relationship:

$$\text{NGl} = \text{number of coefficients in the tax formula} \tag{26}$$

Thus, each gene corresponds to one coefficient of the tax formula. The optimization process is performed in a manner that selects the tax coefficients that yield the highest PSSI as the solution to the problem. The optimization is considered complete when the changes in the cost function become negligible, typically less than 0.1%.

Additionally, the AC-OPF relationships are described below. The objective function in AC-OPF is to minimize the cost of production as follows:

$$\text{Min}\, f(x) \tag{27}$$
$$g(x) = 0 \tag{28}$$
$$h(x) \leq 0 \tag{29}$$
$$x_{min} \leq x \leq x_{max} \tag{30}$$

where, x_{min} and x_{max} are bounds include reference bus angles, voltage magnitudes, and generator injections. The AC-OPF objective function $f(x)$ consists of the non-linear cost of the generator's produced power:

$$f(x) = \sum\nolimits_i (C_{F_i}\left(P_{F_{i,h}}\right) + C_{w_i}(P_{w_i})) \tag{31}$$

The equality constraints $g(x)$ indicate the power balance equations, and the inequality constraints $h(x)$ indicate the branch limits. The x_{min} and x_{max} bounds include reference bus angles, voltage magnitudes, and generator injections. The following constraints are also considered:

$$P_{i,h} - P_{i,h-1} \leq UR_i, \quad i = 1 \ldots n_{F+}n_W \tag{32}$$
$$P_{i,h-1} - P_{i,h} \leq DR_i, \quad i = 1 \ldots n_{F+}n_W \tag{33}$$
$$P_{i,total} = P_{d,total} + P_{l,total} \tag{34}$$
$$Q_{i,total} = Q_{d,total} + Q_{l,total} \tag{35}$$
$$\theta_i^{ref} \leq \theta_i \leq \theta_i^{ref}, \quad i = 1 \ldots b \tag{36}$$
$$v_m^{i,min} \leq v_m^i \leq v_m^{i,max}, \quad i = 1 \ldots n_{F+}n_W \tag{37}$$
$$p_g^{i,min} \leq p_g^i \leq p_g^{i,max}, \quad i = 1 \ldots n_{F+}n_W \tag{38}$$
$$q_g^{i,min} \leq q_g^i \leq q_g^{i,max}, \quad i = 1 \ldots n_{F+}n_W. \tag{39}$$

where, UR_i and DR_i are ramp up and ramp down limits of i^{th} producer, $P_{i,total}$ and $Q_{i,total}$ are total active and reactive powers and $P_{d,total}$ and $Q_{d,total}$ are total active and reactive power demands, $P_{l,total}$ and $Q_{l,total}$ are total active and reactive power losses respectively. $v_m^{i,min}$, v_m^i and $v_m^{i,max}$ are minimum, actual, and maximum voltage magnitudes of buses, respectively. $p_g^{i,min}$, p_g^i and $p_g^{i,max}$ are minimum, actual, and maximum active power of producers, and $q_g^{i,min}$, q_g^i and $q_g^{i,max}$ are Minimum, actual, and maximum reactive power of producers, respectively. θ_i^{ref} and θ_i are nodal voltage angle reference and nodal voltage angle of buses respectively. The flowchart of the proposed method is illustrated in Fig. 3.

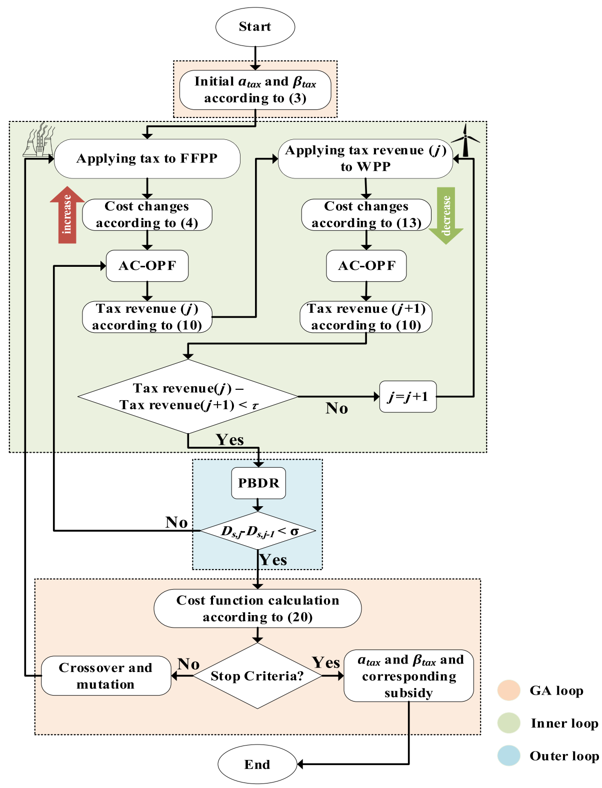

FIGURE 3. Flowchart of the proposed OCTSM.

IV. SIMULATION RESULTS

The study analyzed the IEEE 24-bus test system which included six wind turbines. These wind turbines were located at buses 3, 5, 7, 16, 21, and 23. The layout of the test system is shown in Fig. 4. The detailed parameters of the system can be found in Appendix and [39] and 40. The simulation was conducted using MATLAB R2021a.

This study presents the results for three different scenarios:

First scenario: Six wind turbines with a capacity of 300 MW were operated.

Second scenario: Six wind turbines with a capacity of 350 MW were operated.

Third scenario: Six wind turbines with a capacity of 400 MW were operated.

In all scenarios, the values of F_{CO_2} and R_{CO_2} were 50 \$/ton and 0.4421 ton/MWh respectively. The F_D can be calculated using the elasticity of gross domestic product (GDP) to electricity consumption and the average price of electricity. So, according to [41] it is determined to be 6.74 \$/MWh. The daily mean and variance of wind speed were extracted from reference [42] to calculate the corresponding Weibull distribution parameters. The scenario reduction method proposed in reference [37] was applied to generate 10 wind scenarios representing different wind conditions. The values of demand elasticity were obtained from reference [38].

Fig. 5 displays the convergence diagram of the OCTSM problem. The optimization process continued until the cost function reached a stable state.

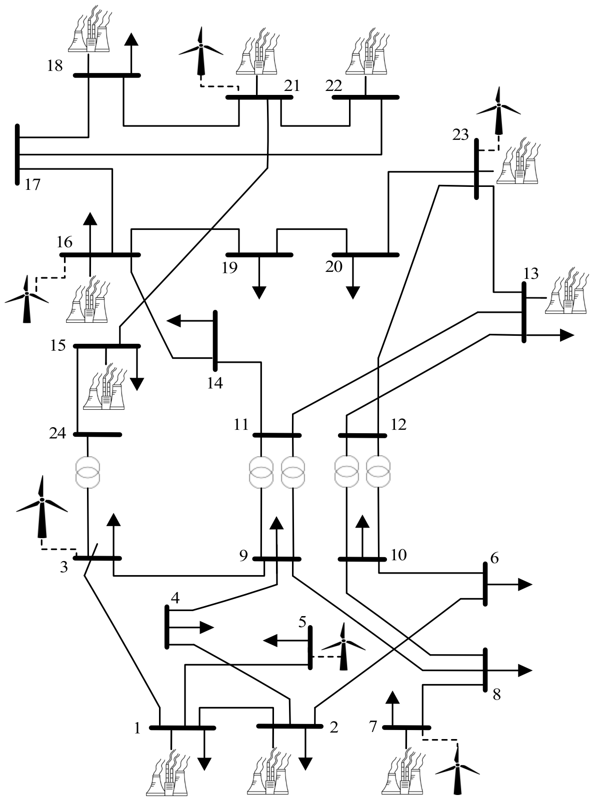

FIGURE 4. Modified IEEE 24-bus test system.

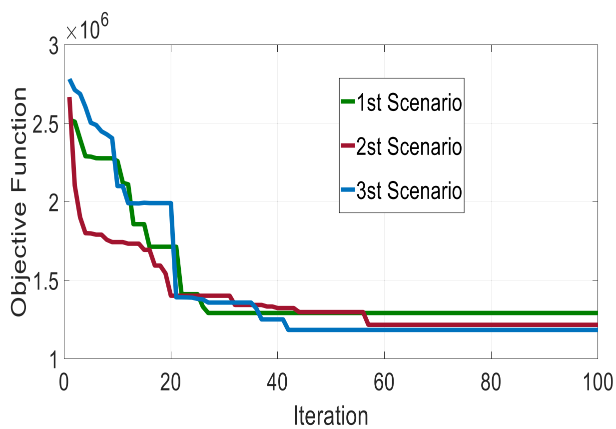

FIGURE 5. Convergence diagrams for all three scenarios in the OCTSM problem.

In other words, Fig. 5 illustrates the optimization process of the cost function (20) by GA in all scenarios. As shown in Fig. 5, the optimization process reaches its optimum point after approximately 60 iterations.

Figs. 6 and 7 present the convergence diagrams for first scenario and 100% subsidy. As shown in Fig. 6, in the first iteration, only the subsidy amount was paid and there was no tax amount. After executing the AC-OPF, the tax amount was obtained and paid as the subsidy amount. This process continued until convergence, where the subsidy and tax amounts became equal. In other words, according to Fig. 2, Fig. 6 illustrates the convergence of the inner loop,

After the initial subsidy, the cost function of WPP change. This alteration impacts the power flow results and alters the amount received from taxes and, consequently, the subsidy amount. This process continues until convergence, meaning the equalization of tax revenues received and subsidies paid, as shown in Fig. 6.

Fig. 7 illustrates the inner loops and the execution location of the outer loop, i.e., according to Fig. 2, following the convergence of the inner loop, the outer loop process initiates. It continues until the outer loop also converges, meaning there is no change in the demand. At the end of the first inner loop (blue diagrams), the first PBDR was performed, resulting in a decrease in the consumption. Then the second inner loop was executed to equalize the tax and subsidy. At the end of this loop, the PBDR was executed for the second time (the second iteration of the outer loop), considering the new network price. After the second PBDR the amount of demand increased compared to the previous state. However, the rate of change in the demand gradually decreased.

As seen in Fig. 7, the difference in the steady state or the subsidy amount after the first PBDR is 4494 dollars, and after the second PBDR is 1967 dollars. Therefore, the outer loop also converged gradually.

Table 2 presents the outputs of the 1st hour corresponding to wind scenarios. The weighted outputs of CO_2 were calculated based on (17). Table 3 displays the numerical results after the system convergence for each scenario. The optimized tax coefficients obtained from (3) are also shown. Table 3 also provides information on the PSSI, calculated using (7) and (20), and its indicators. Figs. 8 and 9 depict the power produced by wind generators at a specific bus under different scenarios and subsidy allocations, as well as the total carbon dioxide production over a 24-hour period for various tax situations. As observed in Fig. 8, the penetration of WPP has increased with the implementation of the proposed approach. Fig. 10 shows the relationship between the PSSI after applying the optimal tax with the capacity of wind generators, CO_2 emissions, and system cost. Fig. 11 illustrates the PSSI of the system buses for each scenario according to (8).

The application of tax in the first scenario results in a 10.95% reduction in carbon dioxide emissions, as indicated in Table 3. Introducing a 10% subsidy for wind producers increases this reduction to 15.42%. However, this case does not significantly decrease the prices of wind producers, leading to decreased PSSI. Allocating a 100% subsidy leads to a 26.42% reduction in carbon dioxide and the cost also decreases due to the large amount of subsidy compared to the prior cases, which results in increased PSSI. These patterns are observed in other scenarios as well.

Additionally, it can be concluded that in the first scenario, the penetration of WPP is insufficient, and wind production reaches its limit. Therefore, the optimization process cannot significantly increase the PSSI beyond a certain level. During

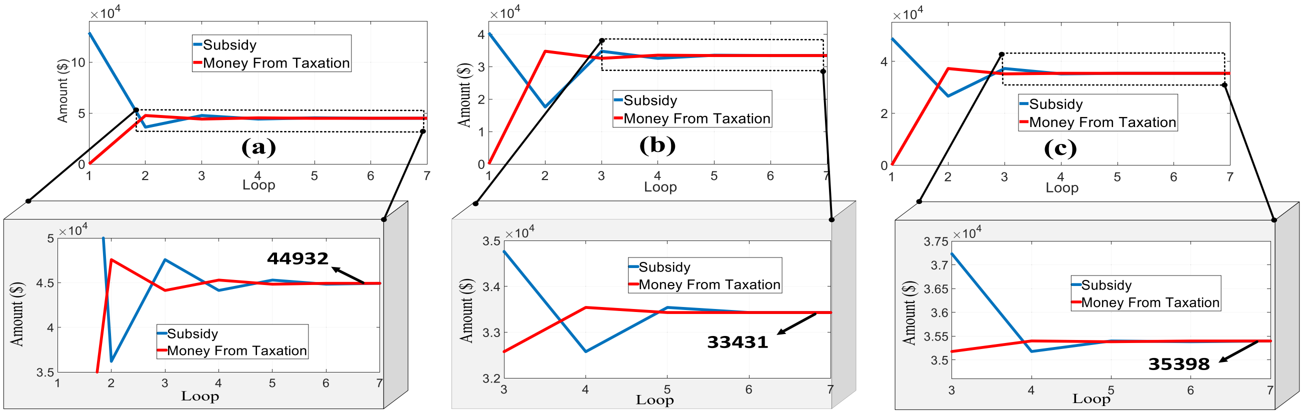

FIGURE 6. Convergence of the amount of tax and subsidy (Inner Loop According to Fig. 2) In 24 Hours to determine the operating point at first scenario and 100% Subsidy Case. A: 1st Inner Loop, B: 2nd Inner Loop, C: 3rd Inner Loop.

TABLE 2. Outputs of 1st hour corresponding to wind scenarios.

Num. of wind scenario	Probability (%)	Max power of WPP in the 1st hour						CO_2 (ton)			
		P_{w_1}	P_{w_2}	P_{w_3}	P_{w_4}	P_{w_5}	P_{w_6}	W/O tax	W/ tax and W/O subsidy	W/ tax and 10% subsidy	W/ tax and 100% subsidy
1	13.86	47.88	43.2	41.13	57.23	20.8	51.6	746.68	745.41	745.17	744.85
2	6.35	26.34	38.94	40.8	33.53	29.03	36.11	748.41	747.52	747.4	747.05
3	2.99	34.12	39.01	59.24	50.91	38.99	42.34	747.61	746.27	745.75	745.1
4	5.6	32.4	36.42	46.32	29.14	19.91	28.41	746.21	745.27	744.33	744.15
5	22.8	56.24	28.94	57.22	38.1	22.82	31.01	746.41	745.31	745.05	744.55
6	1.53	37.5	48.44	38.94	41.03	30.14	26.89	746.88	745.72	745.28	744.04
7	28.22	59.15	24.65	42.11	57.35	33.01	59.02	746.29	745.37	745.08	744.37
8	5.92	42.82	48.91	38.94	46.4	33.86	35.09	746.44	745.63	745.29	744.33
9	10.9	41.76	44.42	33.53	31.1	25.43	38.52	747.92	745.38	744.96	744.22
10	1.83	33.1	58.81	43.92	54.47	30.09	41.89	746.32	745.81	745.13	744.81
		WEIGHTED MEAN						746.74	745.55	745.21	744.64

TABLE 3. Results of the proposed method.

	1ST SCENARIO				2ND SCENARIO			3RD SCENARIO		
	W/O tax	W/ tax and W/O subsidy	W/ tax and 10% subsidy	W/ tax and 100% subsidy	W/ tax and W/O subsidy	W/ tax and 10% subsidy	W/ tax and 100% subsidy	W/ tax and W/O subsidy	W/ tax and 10% subsidy	W/ tax and 100% subsidy
Coefficients	a_{tax}= 0 b_{tax}= 0	a_{tax}= 0.00921 b_{tax}= 0.000401	a_{tax}= 0.01515 b_{tax}= 0.000651	a_{tax}= 0.015301 b_{tax}= 0.00089	a_{tax}= 0.055137 b_{tax}= 0.000519	a_{tax}= 0.072041 b_{tax}= 0.000225	a_{tax}= 0.06243 b_{tax}= 0.00041	a_{tax}= 0.07217 b_{tax}= 0.000381	a_{tax}= 0.080159 b_{tax}= 0.000519	a_{tax}= 0.082721 b_{tax}= 0.000541
CO_2 (ton)	17395.68	15490.771	14712.893	12798.437	15013.962	14233.311	11640.801	13602.376	12821.751	11027.9٥
Change (%)	-	-10.95	-15.42	-26.42	-13.69	-18.17	-33.08	-21.80	-26.29	-36.60
Cost ($)	367439.5	465421.92	456326.03	418411.53	476181.82	468805.56	418581.28	510116.33	498612.18	419442.54
Change (%)	-	26.66	24.19	13.87	29.59	27.58	13.91	38.83	35.69	14.15
LMP ($/MWh)	5.206	6.715	6.58	6.029	6.884	6.765	6.024	7.368	7.193	6.046
Change (%)	-	28.98	26.39	15.80	32.23	29.94	15.71	41.53	38.17	16.13
24-h demand (MWh)	99080. 24	86254.6١١	87253.639	92246.679	84767.876	85479.91	92239.124	79908.72	81461.382	92156.422
PSSI	1	0.864	0.942	1.304	0.869	0.942	1.502	0.874	0.964	1.628
Change (%)	-	-13.6	-5.8	30.4	-13.1	-5.8	50.2	-12.6	-3.6	62.8

peak hours, WPP reached their maximum available power (as seen in Fig. 8 (a) from hours 19 to 21), and increasing tax coefficients only leads to higher prices because a substantial amount of electricity still needs to be supplied by FFPP.

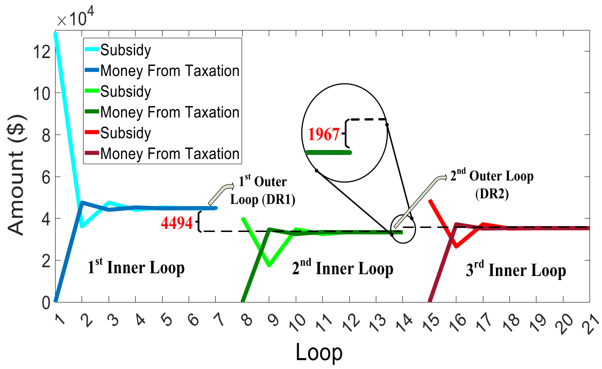

FIGURE 7. Convergence chart of inner and outer loops according to Fig. 2, at first scenario and 100% subsidy case.

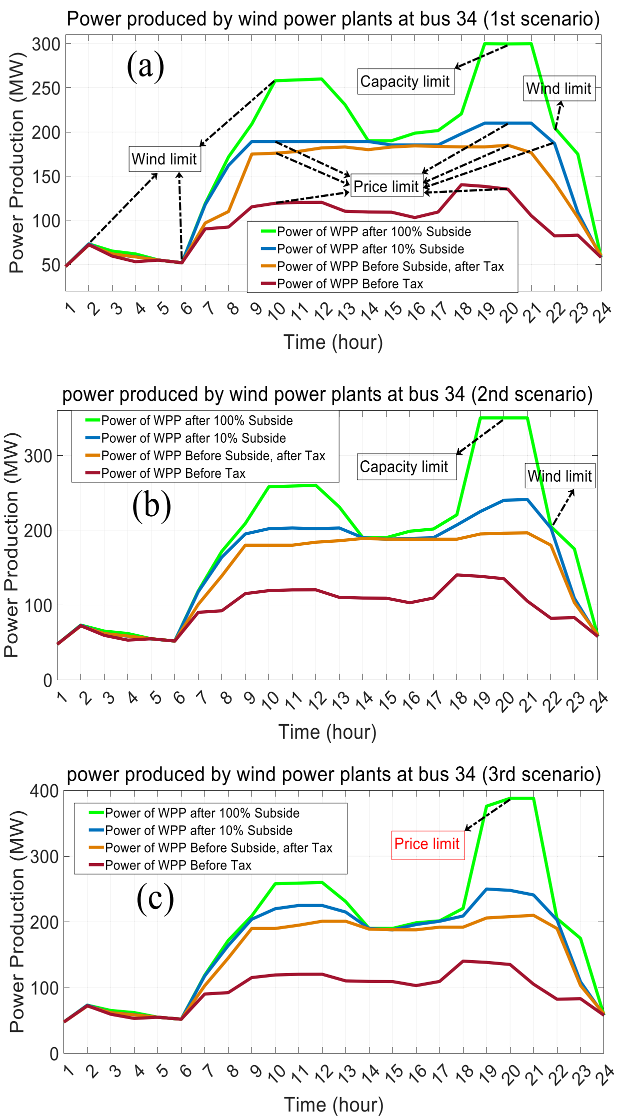

FIGURE 8. Power produced by wind generators at bus 34 in each hour in (a) 1st, (b) 2nd and (c) 3rd scenario.

In the second scenario, with an increased penetration of wind sources, the capacity limit expanded. By enlarging the

FIGURE 9. Total CO_2 in 24 hours in different cases for (a) 1st scenario, (b) 2nd scenario, and (c) 3rd scenario.

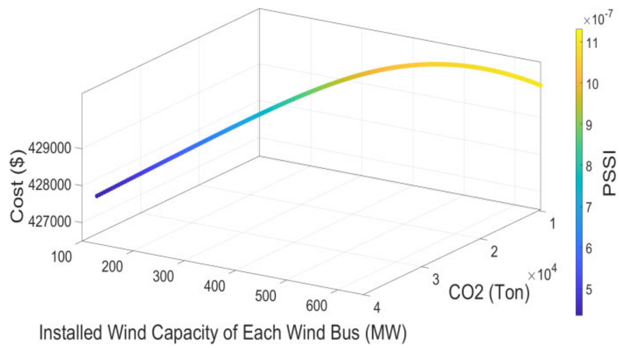

FIGURE 10. The relationship between the PSSI obtained by applying the OCTSM with the installed capacity of wind generators, CO_2 emissions, and system cost.

coefficients of the tax (as it is seen in Table 3), more wind production is utilized. The significant reduction in carbon dioxide offsets the price increase resulting from the enlarged tax coefficients. Moreover, FFPP play a lesser role in power supply, and due to the non-linearity of production, the tax coefficient only acts as a deterrent and has a minor impact on price increases. As the capacity of WPP increases and the tax becomes more stringent, due to the potential for CO_2 reduction, a further increase in wind resource penetration is observed during non-peak hours. In other words, during hours when there is a price limitation (non-competitive price of WPP compared to FFPP), this limitation is partially compensated. For example, at hour 22, after applying subsidy, the price limitation is removed, and wind generation production is constrained by the wind resource limit. Consequently, the second scenario exhibited a substantial increase in the PSSI, as shown in Table 3. In the case of 100% subsidy allocation, the PSSI experiences a significant 50.2% increase, contrasting with the first scenario where the index increased by 30.4%. In the third scenario, wind resource capacity continues to expand, resulting in an increase in the PSSI. However, it is worth noting that the growth rate of the PSSI decreases compared to the second scenario.

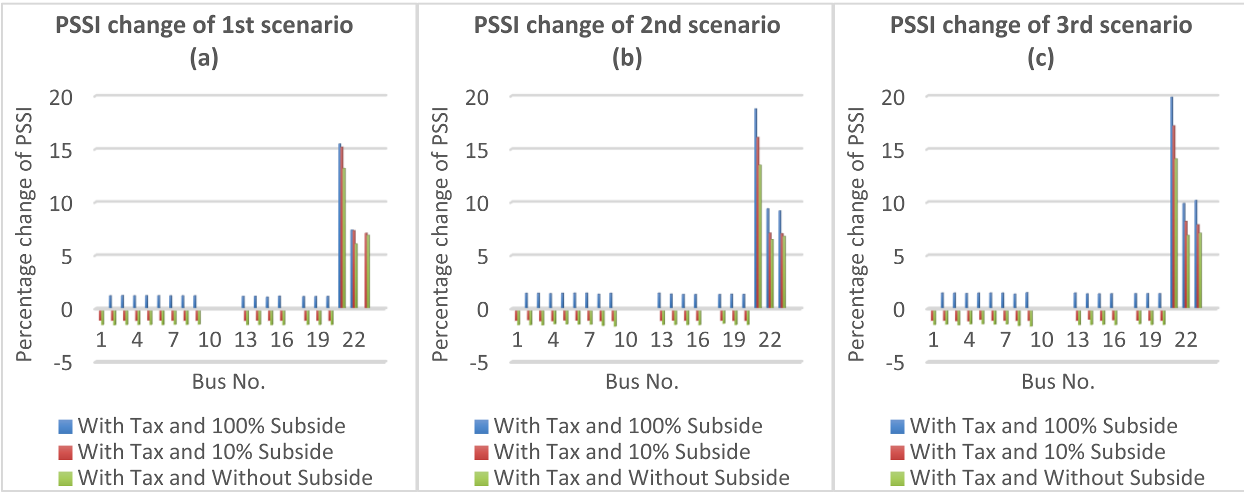

FIGURE 11. PSSI change of each bus in different cases for (a) 1st scenario, (b) 2nd scenario, and (c) 3rd scenario.

TABLE 4. Node location and distribution of the total system demand.

Load #	Node	% of system load	Load #	Node	% of system load
1	1	3.8	10	10	6.8
2	2	3.4	11	13	9.3
3	3	6.3	12	14	6.8
4	4	2.6	13	15	11.1
5	5	2.5	14	16	3.5
6	6	4.8	15	18	11.7
7	7	4.4	16	19	6.4
8	8	6	17	20	4.5
9	9	6.1			

TABLE 5. Technical data of generating units.

Unit	Type	Node	P_i^{max}	P_i^{min}	UR_i /DR_i (MW/h)
1	FFPP	1	152	30.4	120
2	FFPP	2	152	30.4	120
3	WPP	3	300	0	300
4	WPP	5	300	0	300
5	FFPP	7	350	75	350
6	WPP	7	300	0	300
7	FFPP	13	591	206	240
8	FFPP	15	60	12	60
9	FFPP	15	155	54.2	155
10	FFPP	16	155	54.25	155
11	WPP	16	300	0	300
12	FFPP	18	400	100	280
13	FFPP	21	400	100	280
14	WPP	21	300	0	300
15	FFPP	22	300	300	300
16	FFPP	23	310	108	180
17	FFPP	23	350	140	240
18	WPP	23	300	0	300

In the third scenario, the PSSI shows a notable 62.8% increase when a 100% subsidy is allocated, surpassing the increase observed in the previous scenario. However, the growth rate has decreased. In the second scenario, compared to the first scenario, the PSSI has grown by 15.18%. However, in the third scenario, compared to the second scenario, this value has reduced to 8.39%. The decrease in the rate of increase can be attributed to the non-linearity of the cost functions of wind generators, contrasting with the linear reduction of CO_2 and the linear allocation of subsidies. Consequently, at very high penetrations, the rate of increase in PSSI gradually diminishes, and it may no longer be profitable to invest with the intention of increasing PSSI. During hours 19 to 21, the production limit of wind reaches its maximum value due to capacity limitations, as shown in Fig. 8(a). Similarly, in Fig. 8(c), during the same hours, the cost of wind production and the non-linearity of cost functions have limited the production of wind. The impact of the tax on CO_2 reduction has been more apparent in the second scenario, as depicted in Fig. 9 and Table 3.

The results of the sentiment analysis test indicate that PSSI is highly dependent on the capacity of renewable energy sources, carbon dioxide emissions, and energy prices. A 4D diagram in Fig. 10 shows the relationship between wind capacity, emitted CO_2, system cost, and PSSI using curve fitting methods. It can be observed that increasing wind turbine capacity beyond 400 MW does not have a significant effect on increasing PSSI. This limitation is due to the lack of cost-effectiveness in generating more than a specific level from WPP, caused by the non-linear cost function contrasting with the linear subsidy and CO_2 reduction.

In other words, while a sharp increase in the coefficients of the tax formula can raise taxes and subsidies, leading to a decrease in the price of wind turbines and an increase in their

TABLE 6. Cost coefficients of generating units.

Unit	Type	α_i	β_i	γ_i
1	FFPP	0.014142	16.0811	212.3076
2	FFPP	0	130	400.6849
3	WPP	0.02	5	0
4	WPP	0.02	5	0
5	FFPP	0.052672	43.6615	781.521
6	WPP	0.02	5	0
7	FFPP	0.00717	48.5804	831.7575
8	FFPP	0.328412	56.564	86.3852
9	FFPP	0.008342	12.3883	382.2391
10	FFPP	0.008342	12.3883	382.2391
11	WPP	0.02	5	0
12	FFPP	0.000213	4.4231	395.3749
13	FFPP	0.000213	4.4231	395.3749
14	WPP	0.02	5	0
15	FFPP	0	0.001	0.001
16	FFPP	0.008342	12.3883	382.2391
17	FFPP	0.008342	12.3883	382.2391
18	WPP	0.02	5	0

TABLE 7. Load profile.

Hour	System demand (MW)	Hour	System demand (MW)
1	1775.835	13	2517.975
2	1669.815	14	2517.975
3	1590.3	15	2464.965
4	1563.795	16	2464.965
5	1563.795	17	2623.995
6	1590.3	18	2650.5
7	1961.37	19	2650.5
8	2279.43	20	2544.48
9	2517.975	21	2411.955
10	2544.48	22	2199.915
11	2544.48	23	1934.865
12	2517.975	24	1669.815

TABLE 8. Reactance and capacity of transmission lines.

From	To	Reactance (p.u.)	Capacity (MVA)	From	To	Reactance (p.u.)	Capacity (MVA)
1	2	0.0146	175	11	13	0.0488	500
1	3	0.2253	175	11	14	0.0426	500
1	5	0.0907	350	12	13	0.0488	500
2	4	0.1356	175	12	23	0.0985	500
2	6	0.205	175	13	23	0.0884	500
3	9	0.1271	175	14	16	0.0594	500
3	24	0.084	400	15	16	0.0172	500
4	9	0.111	175	15	21	0.0249	1000
5	10	0.094	350	15	24	0.0529	500
6	10	0.0642	175	16	17	0.0263	500
7	8	0.0652	350	16	19	0.0234	500
8	9	0.1762	175	17	18	0.0143	500
8	10	0.1762	175	17	22	0.1069	500
9	11	0.084	400	18	21	0.0132	1000
9	12	0.084	400	19	20	0.0203	1000
10	11	0.084	400	20	23	0.0112	1000
10	12	0.084	400	21	22	0.0692	500

generation, this is not feasible due to the excessive increase in the price of high power production from wind and the LMP of buses, especially those with minimum power generation constraints from FFPP. Hence, the optimization process does not increase the coefficients of the tax beyond a certain limit. Furthermore, Fig. 11 reveals that the increase in the PSSI after applying a 100% subsidy is not very significant in some buses. This is because there are constraints on the minimum production of FFPP in these buses, preventing a decrease in this plant's production beyond a certain level. Additionally, in some areas, the PSSI decreases after the application of the tax due to an increase in the LMP and the lack of a cost-effective alternative (insufficient wind capacity which is already utilized in other buses). Although there is a reduction in CO_2, the price increase in these buses is more significant. However, the overall PSSI of the system has increased, as indicated in Table 3.

V. CONCLUSION

This study focused on an OCTSM to enhance PSSI by accurately defining the objective function and applying optimization techniques. The iterative process of adjusting the tax and subsidies as inner loop, leads to convergence where subsidy payments equal tax received. Also, an outer iterative loop was converged to stabilize the consumption according to the PBDR. Through the coordinated operation of the inner and outer loops, the study successfully obtained an OCTSM. The analysis reveals the following findings: Wind speed, prices, capacity limits of wind sources, and constraints on the minimum production of FFPP significantly affect the penetration of WPP and, consequently, PSSI. The interrelation between capacity and price plays a crucial role, as increasing capacity not only reduces limitations but also enhances price competitiveness through optimal tax-subsidy system. Also, OCTSM have a greater impact on increasing PSSI when there is higher capacity of WPP. To further boost their capacities, incentives can be considered. However, as the total installed capacity increases, the impact on PSSI gradually diminishes, following an exponential-like function.

To further increase PSSI, it is recommended to reduce constraints on the minimum production of FFPP and solve non-linear subsidy allocation. By considering these findings and taking appropriate actions, we can ensure a continuous and sustainable enhancement of the energy system.

APPENDIX

The parameters of IEEE 24-bus test system are listed in Tables 4 to 8.

REFERENCES

[1] P. H. M. M. Feron, "Introduction," in *Absorption-Based Post-Combustion Capture of Carbon Dioxide*. Amsterdam, The Netherlands: Elsevier, 2016, pp. 3–12, doi: 10.1016/b978-0-08-100514-9.00001-9.

[2] Y. Cheng, N. Zhang, Y. Wang, J. Yang, C. Kang, and Q. Xia, "Modeling carbon emission flow in multiple energy systems," *IEEE Trans. Smart Grid*, vol. 10, no. 4, pp. 3562–3574, Jul. 2019, doi: 10.1109/TSG.2018.2830775.

[3] C. Kang, T. Zhou, Q. Chen, J. Wang, Y. Sun, Q. Xia, and H. Yan, "Carbon emission flow from generation to demand: A network-based model," *IEEE Trans. Smart Grid*, vol. 6, no. 5, pp. 2386–2394, Sep. 2015, doi: 10.1109/TSG.2015.2388695.

[4] A. Akbari-Dibavar, B. Mohammadi-Ivatloo, K. Zare, T. Khalili, and A. Bidram, "Economic-emission dispatch problem in power systems with carbon capture power plants," *IEEE Trans. Ind. Appl.*, vol. 57, no. 4, pp. 3341–3351, Jul. 2021, doi: 10.1109/TIA.2021.3079329.

[5] Y. Cheng, N. Zhang, B. Zhang, C. Kang, W. Xi, and M. Feng, "Low-carbon operation of multiple energy systems based on energy-carbon integrated prices," *IEEE Trans. Smart Grid*, vol. 11, no. 2, pp. 1307–1318, Mar. 2020, doi: 10.1109/TSG.2019.2935736.

[6] M. H. Hassan, S. Kamel, and A. G. Hussien, "Optimal power flow analysis considering renewable energy resources uncertainty based on an improved wild horse optimizer," *IET Gener., Transmiss. Distrib.*, vol. 17, no. 16, pp. 3582–3606, Aug. 2023, doi: 10.1049/gtd2.12900.

[7] D. J. Olsen, N. Zhang, C. Kang, M. A. Ortega-Vazquez, and D. S. Kirschen, "Planning low-carbon campus energy hubs," *IEEE Trans. Power Syst.*, vol. 34, no. 3, pp. 1895–1907, May 2019, doi: 10.1109/TPWRS.2018.2879792.

[8] A. Azam, M. Rafiq, M. Shafique, and J. Yuan, "An empirical analysis of the non-linear effects of natural gas, nuclear energy, renewable energy and ICT-Trade in leading CO_2 emitter countries: Policy towards CO_2 mitigation and economic sustainability," *J. Environ. Manag.*, vol. 286, May 2021, Art. no. 112232.

[9] P. Zhang and H. Wang, "Do provincial energy policies and energy intensity targets help reduce CO_2 emissions? Evidence from China," *Energy*, vol. 245, Apr. 2022, Art. no. 123275.

[10] Qin Yirong, "Does environmental policy stringency reduce CO_2 emissions? Evidence from high-polluted economies," *J. Cleaner Prod.*, vol. 341, Mar. 2022, Art. no. 130648.

[11] M. J. Karimi and S. Vaez-Zadeh, "An agent-based model for electric energy policy assessment," *Electr. Power Syst. Res.*, vol. 192, Mar. 2021, Art. no. 106903.

[12] W. McKibbin, A. Morris, P. Wilcoxen, and Y. Cai, "The potential role of a carbon tax in U.S. fiscal reform," Brookings Inst., Washington, DC, USA, Tech. Rep., 2012.

[13] T. Dinan, "Effects of a carbon tax on the economy and the environment," Congressional Budget Office, Washington, DC, USA, Tech. Rep. 4532, May 2013.

[14] J. J. Conti, P. D. Holtberg, J. R. Diefenderfer, S. A. Napolitano, M. Schall, J. T. Turnure, and L. D. Westfall, "Annual energy outlook 2014," U.S. Energy Inf. Admin., Washington, DC, USA, Tech. Rep., 2014.

[15] Z. Liu, B. Hu, Y. Zhao, L. Lang, H. Guo, K. Florence, and S. Zhang, "Research on intelligent decision of low carbon supply chain based on carbon tax constraints in human-driven edge computing," *IEEE Access*, vol. 8, pp. 48264–48273, 2020, doi: 10.1109/ACCESS.2020.2978911.

[16] C.-H. Yang, "A hybrid optimisation decision model for a smart green energy industry park: Exploring the impact of the carbon tax policy in Taiwan," *Comput. Ind. Eng.*, vol. 160, Oct. 2021, Art. no. 107567.

[17] X. He, W. Qi, and X. Tang, "Research on intelligent decision of low carbon supply chain based on carbon tax constraints in human-driven edge computing," *IEEE Access*, vol. 8, pp. 103833–103847, 2020, doi: 10.1109/ACCESS.2020.2999410.

[18] G. Xu and D. Yue, "Pricing decisions in a supply chain consisting of one manufacturer and two retailers under a carbon tax policy," *IEEE Access*, vol. 9, pp. 18935–18947, 2021, doi: 10.1109/ACCESS.2021.3054776.

[19] I. T. Emami, M. MollahassaniPour, M. R. N. Kalhori, and M. S. Deilami, "Short-run economic–environmental impacts of carbon tax on bulk electric systems," *Sustain. Energy, Grids Netw.*, vol. 26, Jun. 2021, Art. no. 100480.

[20] D. J. Olsen, Y. Dvorkin, R. Fernández-Blanco, and M. A. Ortega-Vazquez, "Optimal carbon taxes for emissions targets in the electricity sector," *IEEE Trans. Power Syst.*, vol. 33, no. 6, pp. 5892–5901, Nov. 2018, doi: 10.1109/TPWRS.2018.2827333.

[21] Q. Shi, H. Ren, W. Cai, and J. Gao, "How to set the proper level of carbon tax in the context of Chinese construction sector? A CGE analysis," *J. Cleaner Prod.*, vol. 240, Dec. 2019, Art. no. 117955.

[22] G. Fang, K. Yang, L. Tian, and Y. Ma, "Can environmental tax promote renewable energy consumption—An empirical study from the typical countries along the belt and road," *Energy*, vol. 260, Dec. 2022, Art. no. 125193, doi: 10.1016/j.energy.2022.125193.

[23] L. Li and S. Yu, "Optimal management of multi-stakeholder distributed energy systems in low-carbon communities considering demand response resources and carbon tax," *Sustainable Cities Soc.*, vol. 61, Oct. 2020, Art. no. 102230.

[24] O. D. Melgar-Dominguez, M. Pourakbari-Kasmaei, M. Lehtonen, and J. R. S. Mantovani, "Voltage-dependent load model-based short-term distribution network planning considering carbon tax surplus," *IET Gener., Transmiss. Distrib.*, vol. 13, no. 17, pp. 3760–3770, Sep. 2019, doi: 10.1049/iet-gtd.2018.6612.

[25] H. Park and R. Baldick, "Stochastic generation capacity expansion planning reducing greenhouse gas emissions," *IEEE Trans. Power Syst.*, vol. 30, no. 2, pp. 1026–1034, Mar. 2015, doi: 10.1109/TPWRS.2014.2386872.

[26] X. Chen, J. Lv, M. B. McElroy, X. Han, C. P. Nielsen, and J. Wen, "Power system capacity expansion under higher penetration of renewables considering flexibility constraints and low carbon policies," *IEEE Trans. Power Syst.*, vol. 33, no. 6, pp. 6240–6253, Nov. 2018, doi: 10.1109/TPWRS.2018.2827003.

[27] A. Abuzayed and N. Hartmann, "MyPyPSA-Ger: Introducing CO_2 taxes on a multi-regional myopic roadmap of the German electricity system towards achieving the 1.5 °C target by 2050," *Appl. Energy*, vol. 310, Mar. 2050, Art. no. 118576.

[28] A. Entezari, M. Bahari, A. Aslani, S. Ghahremani, and F. Pourfayaz, "Systematic analysis and multi-objective optimization of integrated power generation cycle for a thermal power plant using Genetic algorithm," *Energy Convers. Manag.*, vol. 241, Aug. 2021, Art. no. 114309.

[29] S. Ma, L. L. Zhang, and X. Cai, "Optimizing joint technology selection, production planning and pricing decisions under emission tax: A Stackelberg game model and nested genetic algorithm," *Expert Syst. With Appl.*, vol. 238, Mar. 2024, Art. no. 122085.

[30] W. Xie, J. Atherton, J. Bai, F. Farazi, S. Mosbach, J. Akroyd, and M. Kraft, "A nuclear future? Small modular reactors in a carbon tax-driven transition to clean energy," *Appl. Energy*, vol. 364, Jun. 2024, Art. no. 123128.

[31] A. P. Martínez, J. Jara-Alvear, R. J. Andrade, and D. Icaza, "Sustainable development indicators for electric power generation companies in ecuador: A case study," *Utilities Policy*, vol. 81, Apr. 2023, Art. no. 101493.

[32] G. K. Sarangi, A. Mishra, Y. Chang, and F. Taghizadeh-Hesary, "Indian electricity sector, energy security and sustainability: An empirical assessment," *Energy Policy*, vol. 135, Dec. 2019, Art. no. 110964, doi: 10.1016/j.enpol.2019.110964.

[33] Y.-M. Saint-Drenan, R. Besseau, M. Jansen, I. Staffell, A. Troccoli, L. Dubus, J. Schmidt, K. Gruber, S. G. Simões, and S. Heier, "A parametric model for wind turbine power curves incorporating environmental conditions," *Renew. Energy*, vol. 157, pp. 754–768, Sep. 2020, doi: 10.1016/j.renene.2020.04.123.

[34] S. Ageed, N. E. H. Nerweyi, and S. F. Ismael, "Effect of carbon dioxide emitted from private electric generators on health and the environment in the duhok Governorate/Kurdistan region of Iraq," *Ann. Romanian Soc. Cell Biol.*, vol. 25, Apr. 2021, pp. 9024–9032. [Online]. Available: https://annalsofrscb.ro/index.php/journal/article/view/2588

[35] G. E. Metcalf, "On the economics of a carbon tax for the United States," *Brookings Papers Econ. Activity*, vol. 2019, no. 1, pp. 405–484, 2019, doi: 10.1353/eca.2019.0005.

[36] L. Zhang and J. Wei, "Module lifetime evaluation method for the power converter of the DFIG based on the analysis of the field wind speed probability and ambient temperature," *IEEE Access*, vol. 10, pp. 72545–72556, 2022, doi: 10.1109/ACCESS.2022.3189999.

[37] H. Xiao, W. Pei, Z. Dong, L. Kong, and D. Wang, "Application and comparison of metaheuristic and new metamodel based global optimization methods to the optimal operation of active distribution networks," *Energies*, vol. 11, no. 1, p. 85, Jan. 2018, doi: 10.3390/en11010085.

[38] X. Qu, H. Hui, S. Yang, Y. Li, and Y. Ding, "Price elasticity matrix of demand in power system considering demand response programs," *IOP Conf. Ser., Earth Environ. Sci.*, vol. 121, Feb. 2018, Art. no. 052081, doi: 10.1088/1755-1315/121/5/052081.

[39] C. Grigg, P. Wong, P. Albrecht, R. Allan, M. Bhavaraju, R. Billinton, Q. Chen, C. Fong, S. Haddad, S. Kuruganty, W. Li, R. Mukerji, D. Patton, N. Rau, D. Reppen, A. Schneider, M. Shahidehpour, and C. Singh, "The IEEE reliability test system-1996. A report prepared by the reliability test system task force of the application of probability methods subcommittee," *IEEE Trans. Power Syst.*, vol. 14, no. 3, pp. 1010–1020, Aug. 1999, doi: 10.1109/59.780914.

[40] C. Ordoudis, P. Pinson, M. J. M. González, and M. Zugno, ''An updated version of the IEEE RTS 24-bus system for electricity market and power system operation studies,'' Tech. Univ. Denmark, Denmark, 2016, p. 5.

[41] B. Liddle, ''What is the temporal path of the GDP elasticity of energy consumption in OECD countries? An assessment of previous findings and new evidence,'' *Energies*, vol. 15, no. 10, p. 3802, May 2022, doi: 10.3390/en15103802.

[42] S. K. Singh, S. K. Jha, and R. Gupta, ''Enhancing the accuracy of wind speed estimation model using an efficient hybrid deep learning algorithm,'' *Sustain. Energy Technol. Assessments*, vol. 61, Mar. 2024, Art. no. 103603, doi: 10.1016/j.seta.2023.103603.v.

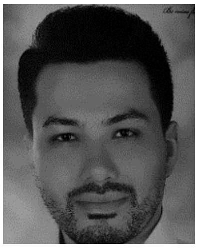

NIMA SHAFAGHATIAN received the M.S. degree from Zanjan University, where he is currently pursuing the Ph.D. degree. He has authored several articles in well-known journals published by IEEE, IET, and Springer. He has also published two books on renewable energy and the relationship between industry and academia subjects. In addition to studying the Ph.D. degree, he is currently a Lecturer with Al-Ghadir University, Zanjan, and offers courses in electrical installations, smart home design, signals and systems, and specialized language of electricity. His research interests include microgrids, power management, and the electricity market.

SEYED HADI HOSSEINI received the B.Sc. degree in power engineering from the University of Tehran, Tehran, Iran, in 1997, and the M.Sc. and Ph.D. degrees in power engineering from Tarbiat Modares University, Tehran, in 2000 and 2005, respectively. He is currently an Assistant Professor with the University of Zanjan, Zanjan, Iran. He has authored several articles in well-known journals and has supervised several research projects in the field of the power system in Iran. His current research interests include planning the development of power grids, designing, troubleshooting, and monitoring of power transformers and power system reliability.

REZA NOROOZIAN received the B.Sc. degree from Tabriz University, Tabriz, Iran, in 2000, and the M.Sc. and Ph.D. degrees in electrical engineering from the Amirkabir University of Technology (AUT), Iran, in 2003 and 2008, respectively. He is currently a Full Professor with the Department of Electrical Engineering, University of Zanjan, Zanjan, Iran. His research interests include power electronics, power systems, power quality, integration and control of renewable generation units, custom power, micro-grid operation, distributed generation modeling, operation, and interface control.